BULLETIN OF THE POLISH ACADEMY OF SCIENCES
TECHNICAL SCIENCES, Vol. 69(3), 2021, Article number: e137055
DOI: 10.24425/bpasts.2021.137055

Bio inspired salamander robot with Pneu-Net Soft actuators – design and walking gait analysis

Elango NATARAJAN[1]*, Kwang Y. CHIA[1], Ahmad Athif Mohd FAUDZI[2], Wei Hong LIM[1], Chun Kit ANG[1], and Ali JAFAARI[2]

[1] Faculty of Engineering, UCSI University, Kuala Lumpur, Malaysia
[2] Center for Artificial Intelligence and Robotics (CAIRO), Universiti Teknologi Malaysia, Kulala Lumpur, Malaysia

Abstract. The research was attempted to mimic the locomotion of the salamander, which is found to be one of the main animals from an evolutionary point of view. The design of the limb and body was started with the parametric studies of pneumatic network (Pneu-Net). Pneu-Net is a pneumatically operated soft actuator that bends when compressed fluid is passed inside the chamber. Finite Element Analysis software, ANSYS, was used to evaluate the height of the chamber, number of chambers and the gap between chambers for both limb and body of the soft mechanism. The parameters were decided based on the force generated by the soft actuators. The assembly of the salamander robot was then exported to MATLAB for simulating the locomotion of the robot in a physical environment. Sine-based controller was used to simulate the robot model and the fastest locomotion of the salamander robot was identified at 1 Hz frequency, 0.3 second of signal delay for limb actuator and negative π phase difference for every contralateral side of the limbs. Shin-Etsu KE-1603, a hyper elastic material, was used to build the salamander robot and a series of experiments were conducted to record the bending angle, the respective generated force in soft actuators and the gait speed of the robot. The developed salamander robot was able to walk at 0.06774 m/s, following an almost identical pattern to the simulation.

Key words: soft actuator; pneumatic network; salamander robot; hyperelastic; parametric study.

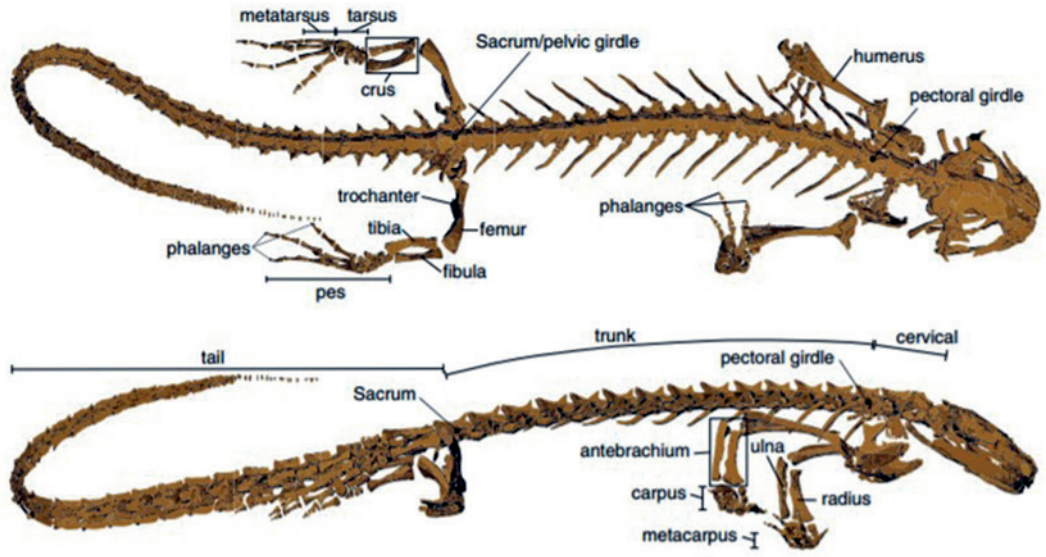

Fig. 1. CT scan image of a salamander [2]

1. Introduction

Animals move in different and rough environments in order to hunt for food, look for mates, run away from predators to survive, etc. The morphologies and central nervous systems of animal focus on controlling their locomotor skills. In recent years, the salamander has caught the attention of researchers as it has the ability to move on different terrains and uneven surfaces. The locomotion of salamanders is controlled by the central pattern generator (CPG) [1]. Figure 1 shows a computed tomography (CT) scan image of a salamander presented by Karakasiliotis *et al.* [2]. It has four limbs and a body that consists of a trunk and tail. The limb forces are used in walking, running or swimming of the animal.

*e-mail: elango@ucsiuniversity.edu.my

Manuscript submitted 2020-09-16, revised 2020-12-20, initially accepted for publication 2020-12-30, published in June 2021

Low-frequency stimulation of CPG induces walking gait whereas high-frequency stimulation changes its gait from walking to swimming [3]. In addition, CPG also controls the speed and direction of locomotion. Edwards [4] reported that the salamander uses two walking styles; one for slow motion and another one for fast walking. It uses lateral sequence walk in slow motion, in which three limbs touch the ground and one provides a forward motion. Fast walking is known as trot, in which two limbs touch the ground and the two other limbs provide the forward motion. The diagonal limbs of the salamander move in synchrony in the trotting gait. During the walking gait, the body of the salamander forms a standing wave where the trunk is maintained at a C-shape curve and it slowly turns straight and eventually changes the curve to the other side [5]. The study of all these locomotion patterns and styles motivates designers and researchers to mimic and develop mechanical robots. Ijspeert *et al.* [6] conducted a neuro-mechanical study of the salamander and attempted to develop the control system accordingly.

Karakasiliotis and Ijspeert [7] later developed Salamandra robotica II that used a CPG controller to manipulate its locomotion. Ijspeert *et al.* [8] demonstrated the switching from walking gait to swimming gait by developing a spinal cord model. Bicanski *et al.* [9] studied the musculoskeletal system and attempted to decode the interaction of CPG. Liu *et al.* [10, 11] developed a spinal locomotor network model using a neural network to build a 3D biomechanical salamander. Zhou *et al.* [12] attempted a dynamic study of CPG for biomimetic robotic fish. Faudzi *et al.* [13] used McKibben muscles to design a salamander robot and investigated robot gait during walking on terrain and swimming in water.

Inspired by the flexible motion of the salamander, a soft mechanism-based salamander robot was attempted to be constructed in this research. Soft actuators are pneumatic actuators made of rubber-like material, which can be linearly or rotationally actuated. There are different kinds of soft actuators designed and used in different applications [14–24]. Ili *et al.* [14] conducted three-dimensional analysis of different designs of reinforced soft actuators and evaluated the designs based on bending actuation. Razif *et al.* [15] applied soft actuators for actuation of robotic fish. Elango *et al.* [16] presented the review of soft materials for robotic applications. The design and actuation forces were investigated in [17–20, 22, 24]. Furukawa *et al.* [21] applied soft actuators to develop the Octopus robotic structure, while Robertson *et al.* [23] applied soft actuators for an origami-inspired modular robot. Cacucciolo *et al.* [22] developed a stretchable pump for soft manipulation. Natarajan *et al.* [24] evaluated Silicone RTV and multiwall carbon nanotubes (MWCNT) reinforced silicone material for soft actuator application and reported that the MWCNT-reinforced soft actuator is better for higher payload.

Mosadegh *et al.* [25] designed a fast pneumatic network, also known as Pneu-Net (fPN) and reported that the rate of actuation by fPN soft actuators is high and reliable. Wang *et al.* [26] attempted to design fPN which can bend and twist.

The current research attempted to design a fast Pneu-Net (fPN) soft actuator for developing limbs and body of the salamander robot. The bending motions of the parts following a certain pattern was the actuation principle for mimicking the locomotion of the salamander. The design of the limb and body actuators was done through parametric studies using finite element analysis (FEA), as presented in section 2.1. The design of the controller and the respective simulation of the salamander robot assembly was done in MATLAB, as presented in section 2.2. The respective design of limb and body soft actuators were followed to complete the salamander robot model and tested as presented in section 2.3.

2. Design of the salamander robot

As far as the salamander is concerned, the body and limbs contribute much to the dynamics. The tail does not contribute to the movement of body, rather than it follows the movement of the body. Considering this fact, the current robot design characterized only the body and limbs of the salamander. The tail part was not considered in the design.

Soft actuators have the advantages of size and compactness, light weight and compliance [27]. They use fluid, mainly compressed air as a working fluid. Compressed air pressurizes the actuator and causes it to perform actuation such as elongation, contraction, bending and twisting. Pneu-Net is a network of small chambers embedded as the soft actuator that can inflate when pressured air is forced into it. This inflation is the key component to produce bending movement in an fPN soft actuator.

The current robot consists of four single channel actuators for the limb and two double channel actuators for the body. When pressurized air is supplied to the limb actuator, the limb actuator bends and pushes the salamander body forward through bending motions. During the slower stepping gait of the salamander, the diagonally opposed limbs are moved together while the body makes S-shaped standing waves with nodes at the girdles [8]. Hence, the limb actuator was actuated in a diagonal pattern, in the sense that the front left limb and rear right limb were actuated first, followed by the front right limb and rear left limb. This produced trotting locomotion of the salamander robot.

The body actuators used in the current design are double channel fPN that can bend in two directions to imitate the locomotion of the salamander. The current model does not include the tail part of the real salamander as it does not assist in the movement of the robot. To produce standing wave that imitates the locomotion of the salamander, the actuators were activated in a diagonal pattern.

The numerical simulations were conducted for two reasons; to design components for soft actuation, and to design the right controller to achieve the motion. The former was carried out in a finite element analysis software, known as ANSYS. The later was carried out with the MATLAB tool.

2.1. Parametric study and design of fPN soft actuators. The bending characteristics of an fPN actuator are generally influenced by the stiffness of the material, geometry of inter-

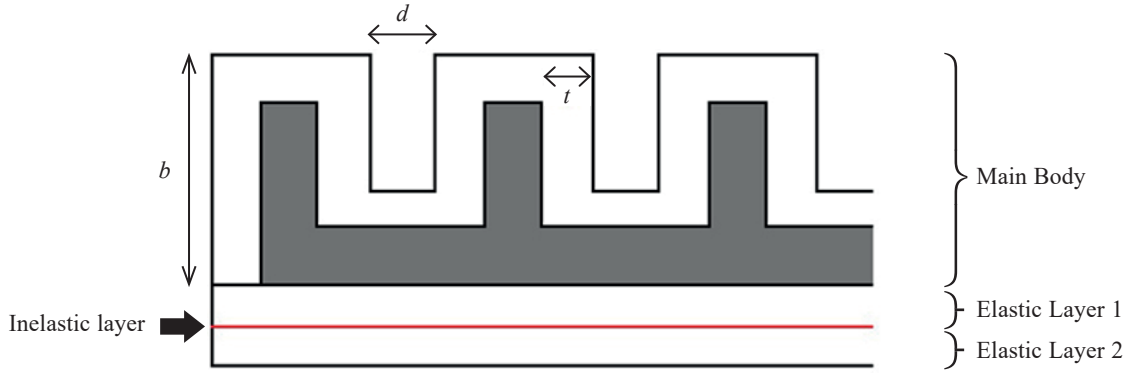

Fig. 2. Schematic diagram of fPN actuator

nal chambers and exterior walls, and the rate of inflation. The fPN has an extensible top layer and inextensible bottom layer, as shown in Fig. 2. The chambers are designed to have two inside walls which have thinner and larger surface areas as compared to the top wall. When pressure is applied, it preferentially expands the inside wall that causes it to push themselves against neighboring chambers and produces a bending actuation. The chamber height (b), wall thickness (t), number of chambers (l) and distance between chambers (d) are main factors influencing the performance of fPN. Hence, parametric studies of these parameters were done through ANSYS to identify the best design parameters.

Finite element analysis and optimization of the design were conducted in [25–29]. Mosadegh *et al.* [25] reported that the rate of actuation is increased by having higher height of the chamber, higher number of chambers and thinner wall thickness. Though the dynamics of the salamander have been investigated in the past, the actual dimensions of the salamander were not presented in any of literatures. Hence, we were not able to follow the exact dimension of the salamander in our current design analysis. Table 1 shows the dimensions considered in the parametric study of the current research. The minimum value in each parameter was fixed based on the mechanical limitations.

Table 1
Dimensions considered in parametric study of the current research

Height of the chamber (mm)	Number of chambers	Thickness of the wall (mm)	Distance between chambers (mm)
15, 18, 21 and 24	4, 5, 6 and 7	1, 1.5, 2 and 2.5	1, 2, 3 and 4

The finite element (FE) models were created according to the selected dimensions. The height of the chamber varied at 15 mm, 18 mm, 21 mm and 24 mm. The number of chambers varied at 4, 5, 6 and 7. The thickness of the wall varied at 1 mm, 1.5 mm, 2 mm and 2.5 mm. The distance between chambers varied at 1 mm, 2 mm, 3 mm and 4 mm. Numerical simulation was carried out for each model. For instance, when the parametric study was conducted for height of the chamber, all other design parameters were a fixed constant. Once the best dimension was found for the particular design parameter, the parametric study was conducted on another parameter. In this manner, the best design parameters were identified.

The meshing details of the limb and body actuator are shown in Table 2. Shin-Etsu KE-1603, a hyper elastic material, was used in all FE models. It is a silicone RTV material with elastic modulus of 1.7338 MPa. Other boundary conditions, such as input pressure, fixed support, gravity and solver time-step, are listed as:

- Input pressure: 80 kPa for limb; 50 kPa for body
- Gravity = 9.8065 m/s^2
- Solver time-step:
  - initial time step = 0.1 s,
  - minimum time step = 0.1 s
  - maximum time step = 0.25 s
- Fixed support at one end of the actuator.

Table 2
Meshing details for limb and body actuators

	Limb	Body
Physics preference	Explicit	Explicit
Element order	Quadratic	Quadratic
Element size	3.0 mm	5.0 mm
Number of elements	4720	4484
Number of nodes	11754	11309

In each simulation, the respective deformation, bending angle and actuation force were recorded. Figure 3 shows a sample result of the numerical simulation-deformation of the body and limb actuators at 20 kPa and the force generated by the body actuator (height = 15 mm).

The best dimensions of body and limb actuators were decided from the model which produced the highest actuation force. The forces generated by the body and limb soft actuators

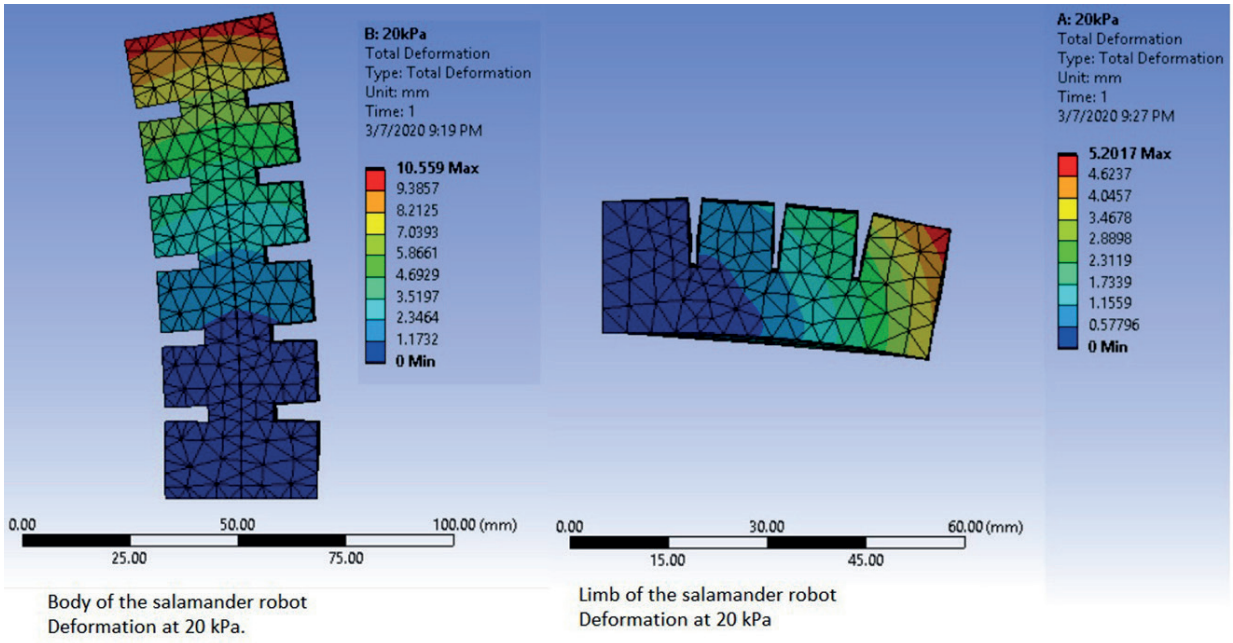

Body of the salamander robot
Deformation at 20 kPa.

Limb of the salamander robot
Deformation at 20 kPa

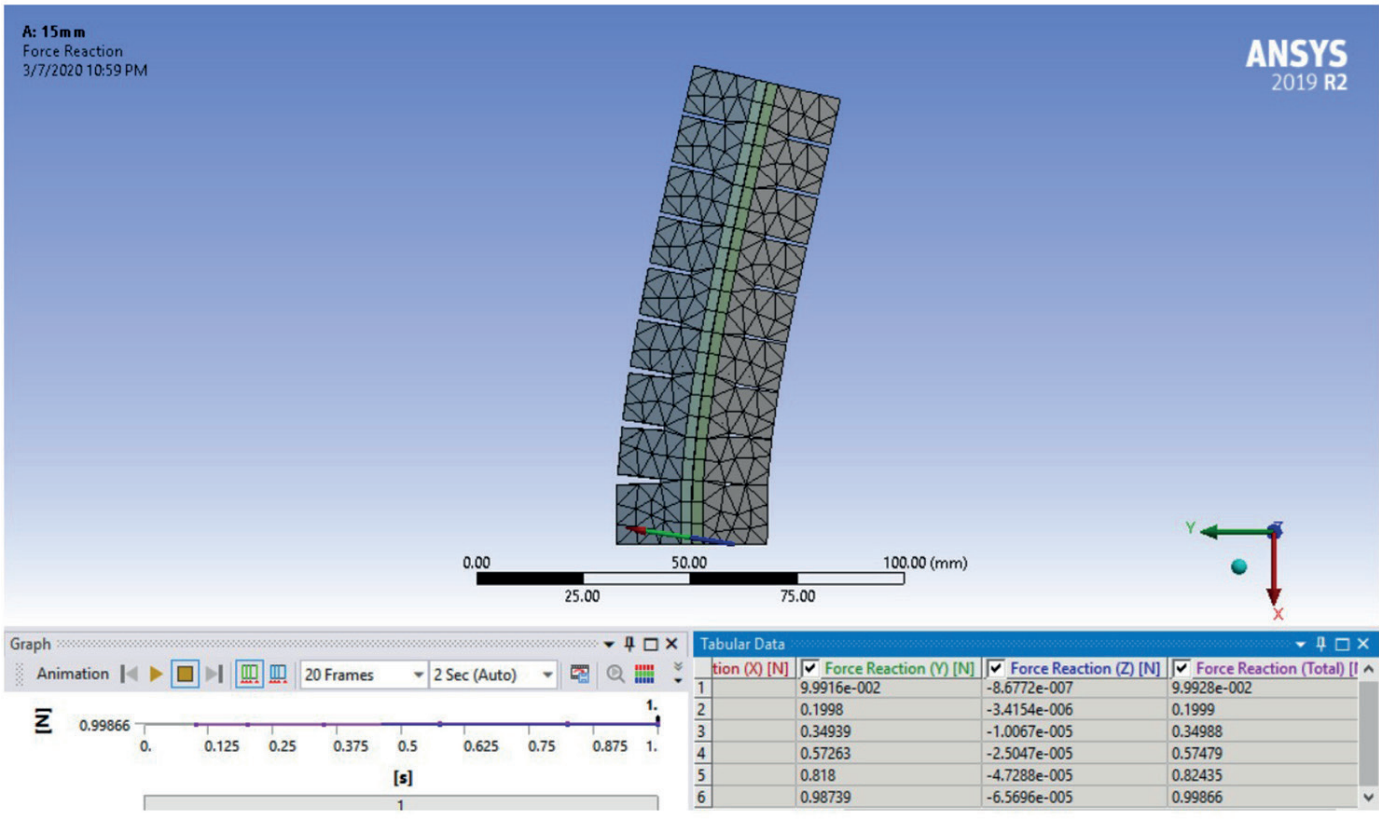

Fig. 3. Deformation of body and limb soft actuators at 20 kPa and force diagram of body actuator (15 mm in height)

are plotted in Fig. 4. From the numerical simulations, a few valuable points are drawn. The actuation force is decreased as the height of the chamber increases. The best force of 5.1256 N and 0.99866 N resulted from fPN actuators of $b = 15$ mm. As far as wall thickness (t) is concerned, the thicker the wall of the chamber, the higher the force generated. The wall thickness of 2.5 mm is the best dimension for both body and limb actuators. As far as the distance between chambers (d) is concerned, the limb and body soft actuator shows results contradicting with each other. The force generated by a limb soft actuator decreases as the distance between the chambers is increased. On the other hand, the force generated by the body actuator

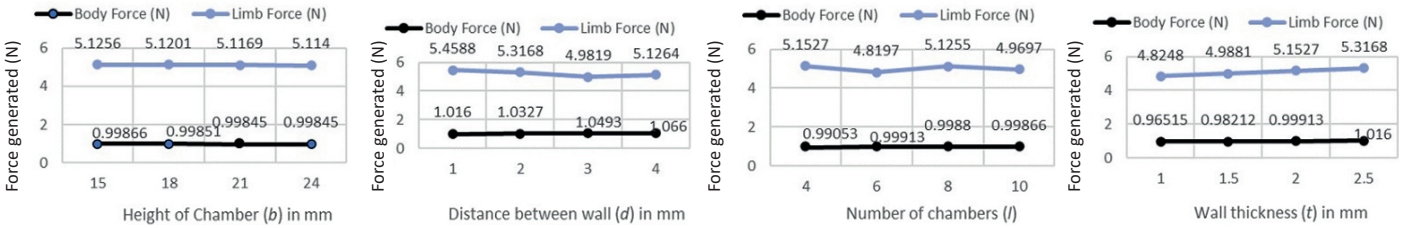

Fig. 4. Simulation results – force generated by body and limb soft actuators

increases as the distance between chambers is increased. In the current design, the limb needs to bend in only one direction, thus only one single channel fPN actuator was used in the design. The body needs to bend in two directions (left and right) and hence dual channel fPN actuators were used in the design. When the body soft actuator bends, the chambers on the opposite side will collide with each other if the distance between the chambers is small. If there is a wide distance between the chambers, there will be more room space for the opposite chamber to bend, and hence the chance of a collision will become less possible. This could be the reason for the body soft actuator to generate more force when there is more space between the chambers. As far as the number of chambers (l) is concerned, the best force was produced by the limb actuator of 4 chambers and the body actuator of 6 chambers. Table 3 shows the finalized parameters for building limb and body actuators.

Table 3
Finalized parameters for salamander limb and body soft actuator

Part	Height of chamber	Number of chambers	Wall thickness	Distance between chambers
Limb	15 mm	4	2.5 mm	1 mm
Body	15 mm	6	2.5 mm	4 mm

2.2. Multibody analysis in MATLAB. In order to simulate and study the walking style of the salamander robot in a physical environment, numerical simulation was conducted with Simscape Multibody in Simulink. With the dimensions finalized in Section 2.1, the salamander robot assembly model was created. The robot model was a solid rectangular block with a body and four limbs. The mass of each part was taken from ANSYS simulations. Figure 5 and Fig. 6 show the finalized salamander robot

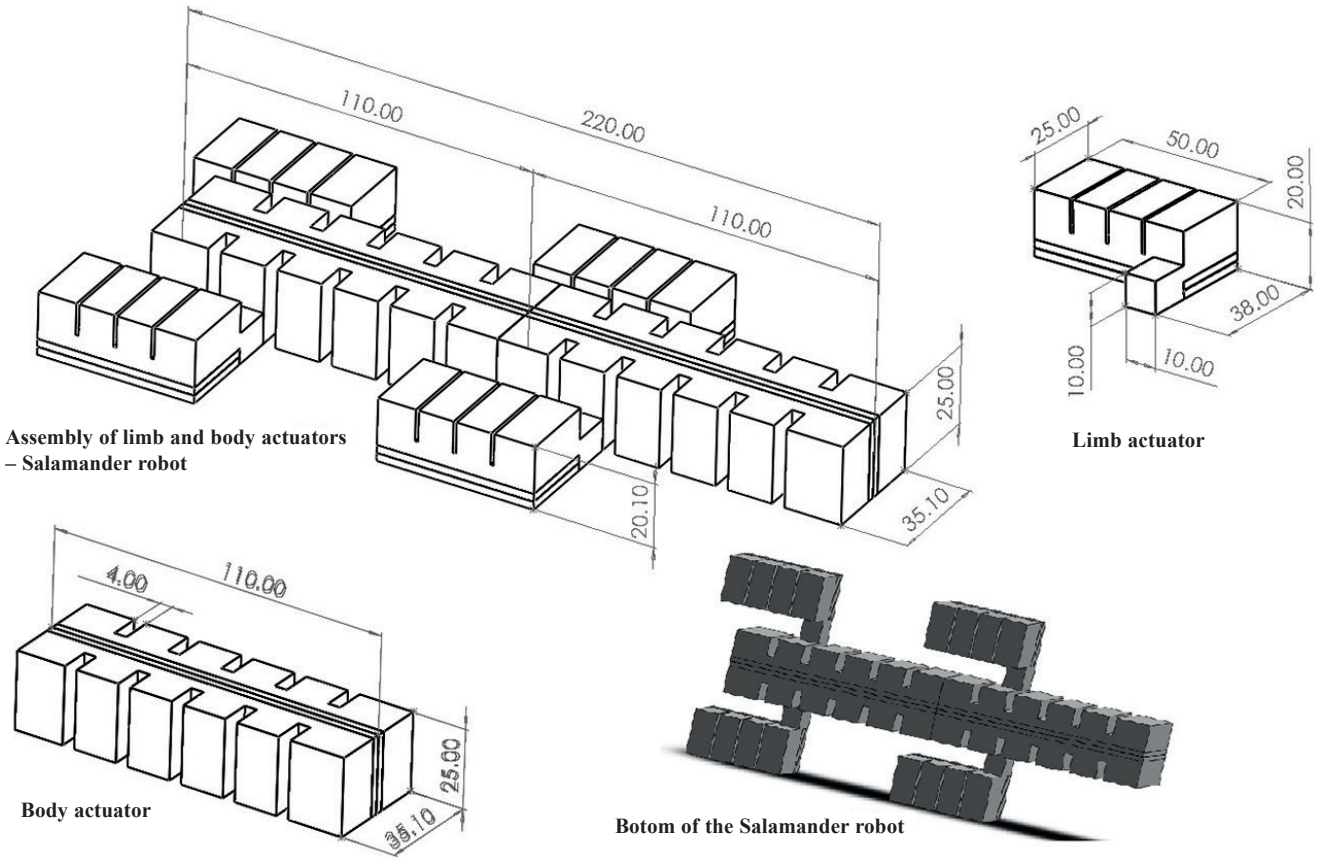

Fig. 5. Finalized salamander robot

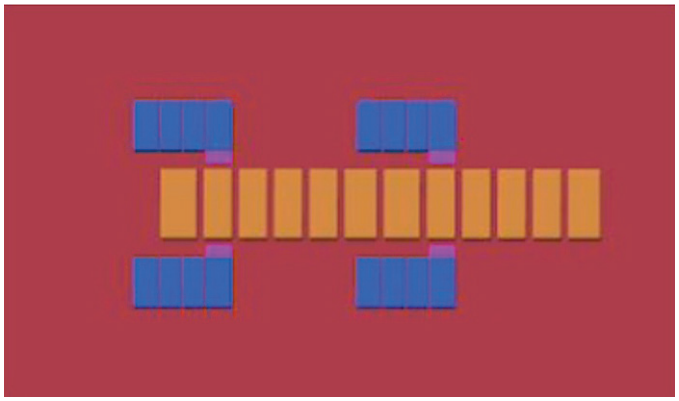

Fig. 6. Model used in MATLAB simulations

and the model used in MATLAB simulation, respectively. The red color ground in Fig. 6 represents the physical flat ground for the robot to move. The torque of 0.138 Nm and 0.11 Nm was applied to the limbs and body, respectively. The torque was controlled by a simple sine-based controller with frequency of 1 Hz. The values of spring stiffness and damping coefficient were computed by the trial-and-error method. The spring stiffness and damping coefficient were tuned to imitate the bending angle and displacement observed in ANSYS simulations. The finalized spring stiffness for limb joint was 1.5 Nm/rad and damping coefficient was 0.015 Nm/(rad/s). As for the body joint, the spring stiffness was 1 Nm/rad and damping coefficient was 0.01 Nm/(rad/s). Furthermore, the controller was fine-tuned to get the fastest locomotion of the salamander robot. The fine tuning was done by means of delaying or advancing the actuation timing between body and limb. After a lot of different settings had been attempted, the fastest locomotion of the salamander was achieved from 1 Hz frequency, 0.3 second of signal delay for limb actuator and negative π phase difference for every contralateral side of the limbs. Fastest velocity of the salamander robot was recorded as 0.07045 m/s at 10 seconds. The estimation of velocity is one of the key factors in designing and constructing walking robots [30].

2.3. Fabrication of soft actuators and salamander robot. The mold for a soft actuator requires three parts: internal extensible layer mold, external extensible layer mold and bottom inextensible mold. In order to fabricate the fPN soft actuators, firstly, mold models were prepared, using Solidworks, and then 3D-printed using acrylonitrile butadiene styrene (ABS) material. A predefined quantity of the curing agent was thoroughly mixed with a predefined quantity of the Shin-Etsu KE-1603 material. The mixture of silicone RTV base material and the curing agent was then poured into the extensible layer (top layer) and inextensible layer (bottom layer). The rotary vacuum pump VRI-2 was used for 30 minutes to degas the silicone mixture in the molds. After ensuring that there were no bubbles in either mold, the molds were placed in an electronic oven (RedLine Binder RF53) to heat them at 80°C for 30 minutes. Once the curing of the molds was confirmed, a piece of butter paper was placed on the inextensible layer and the silicone mixture was further poured to the remaining depth of the mold. The paper served as an inextensible material. The curing of the inextensible layer was done for 30 minutes at 80°C, after which the top and bottom layer were attached together by applying a thin layer of silicone mixture. This made the top layer and bottom layer to become joined together as a single elastomer. Finally, the actuator was removed from the mold and cooled for about 1 hour in room temperature. Figure 7 shows the fabrication of fPN soft actuators.

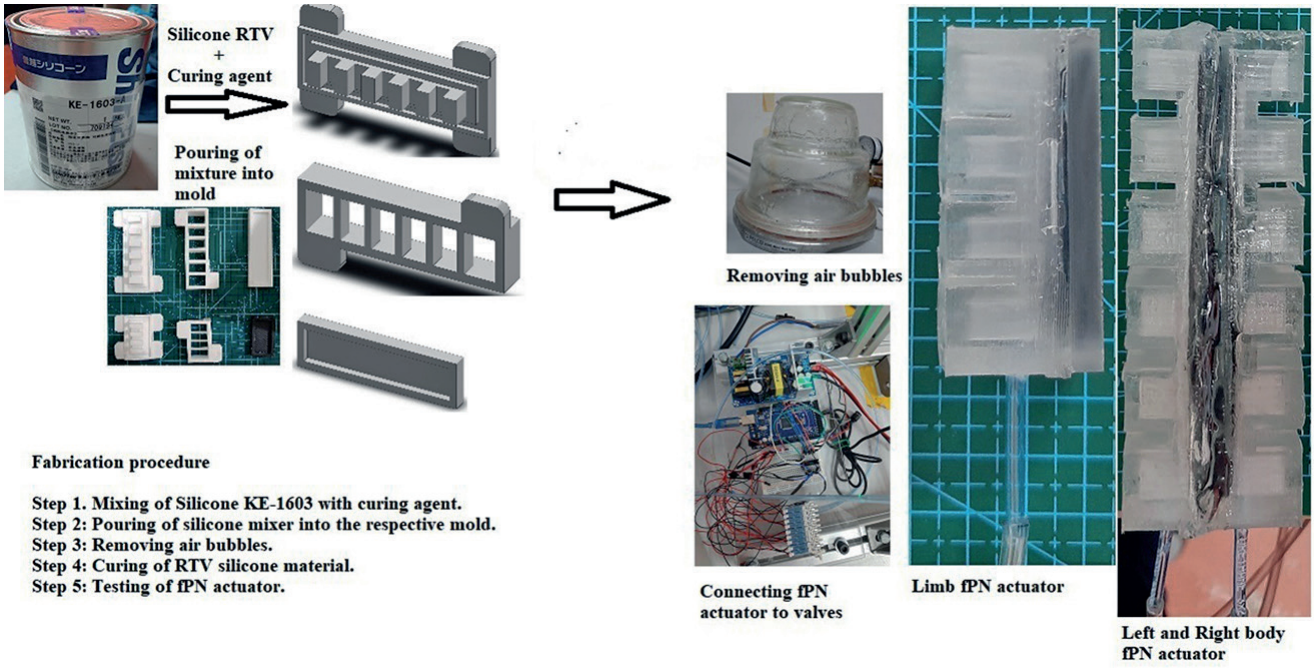

Fig. 7. Fabrication procedure

Once the soft actuators were fabricated, they were experimentally tested at different pressures, as shown in Figure 8, and the corresponding displacement and bending angles were measured and recorded. The comparison of these results with numerical simulation is presented in Section 3.

After confirming the functioning of soft actuators, they were assembled together as a salamander robot. The salamander robot was experimentally tested on a ground with compressed air input through pneumatic valves. Arduino UNO controller, the same as the sine-based controller, was used to control the movement of the robot. A 12V, a 16 channel relay module was used to control the opening and closing of pneumatic valves. The salamander robot was tested at different pressure levels and the speed of the robot was measured and validated against the simulation results. Figure 8 shows the testing of limb actuators and body actuators.

(a)

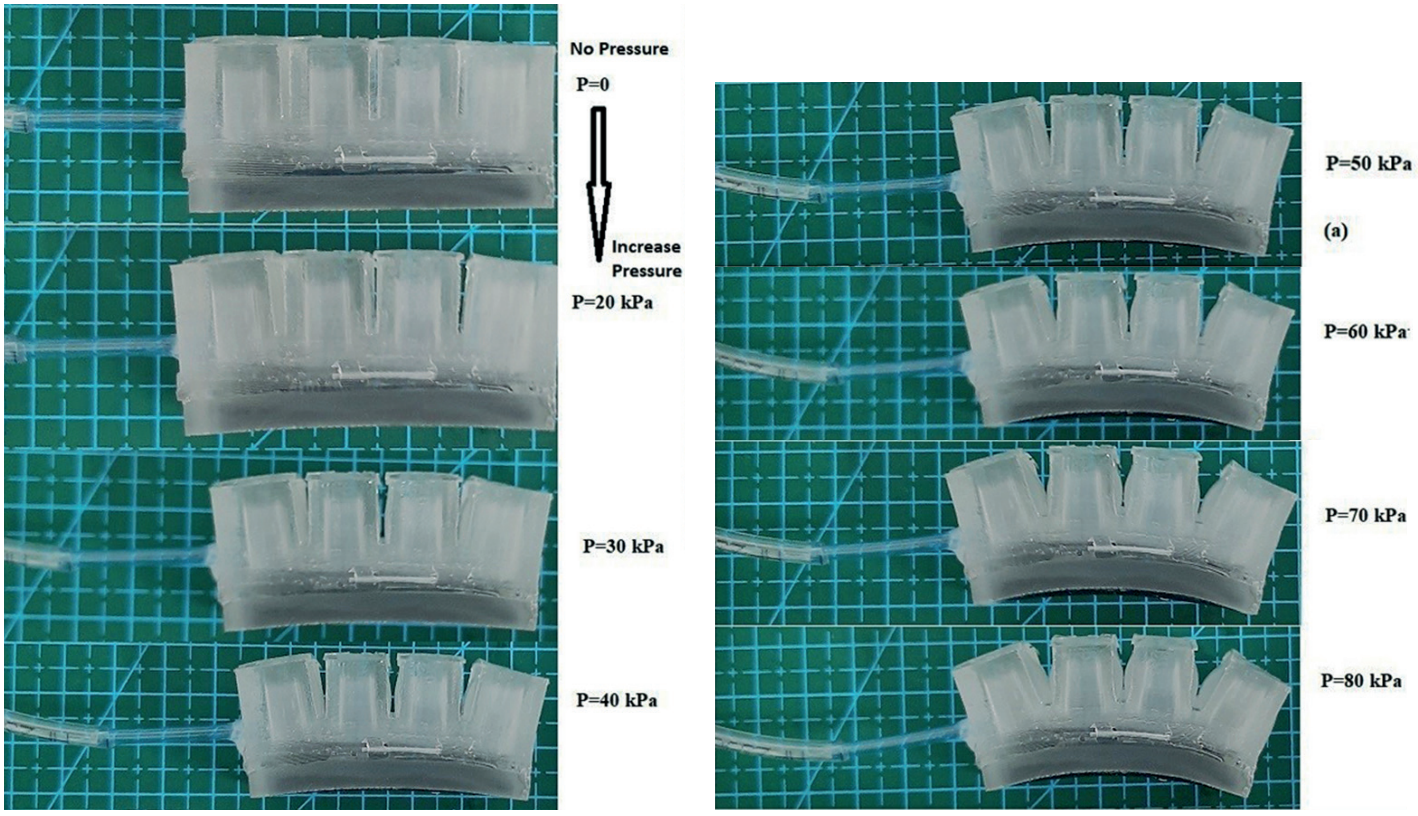

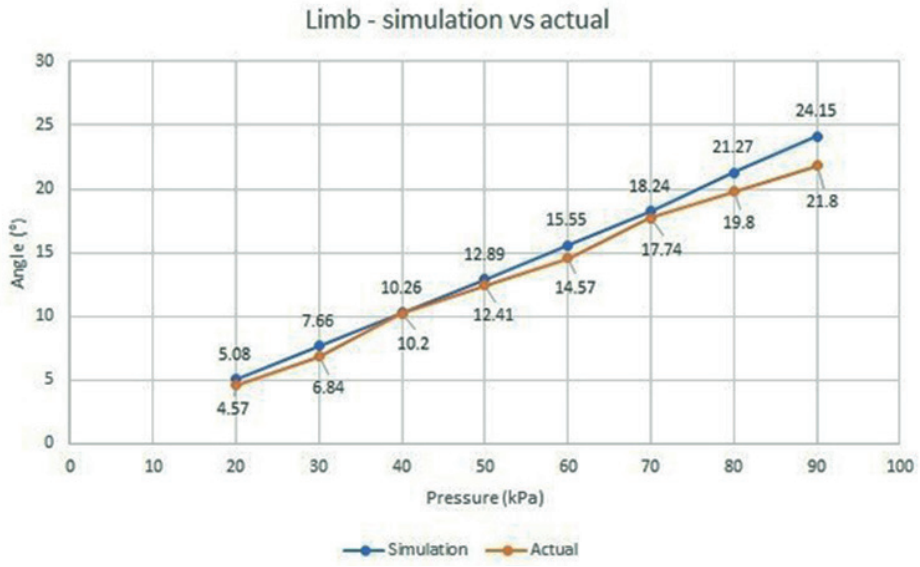

Fig. 8a. Testing of limb actuator at different pressures

(b)

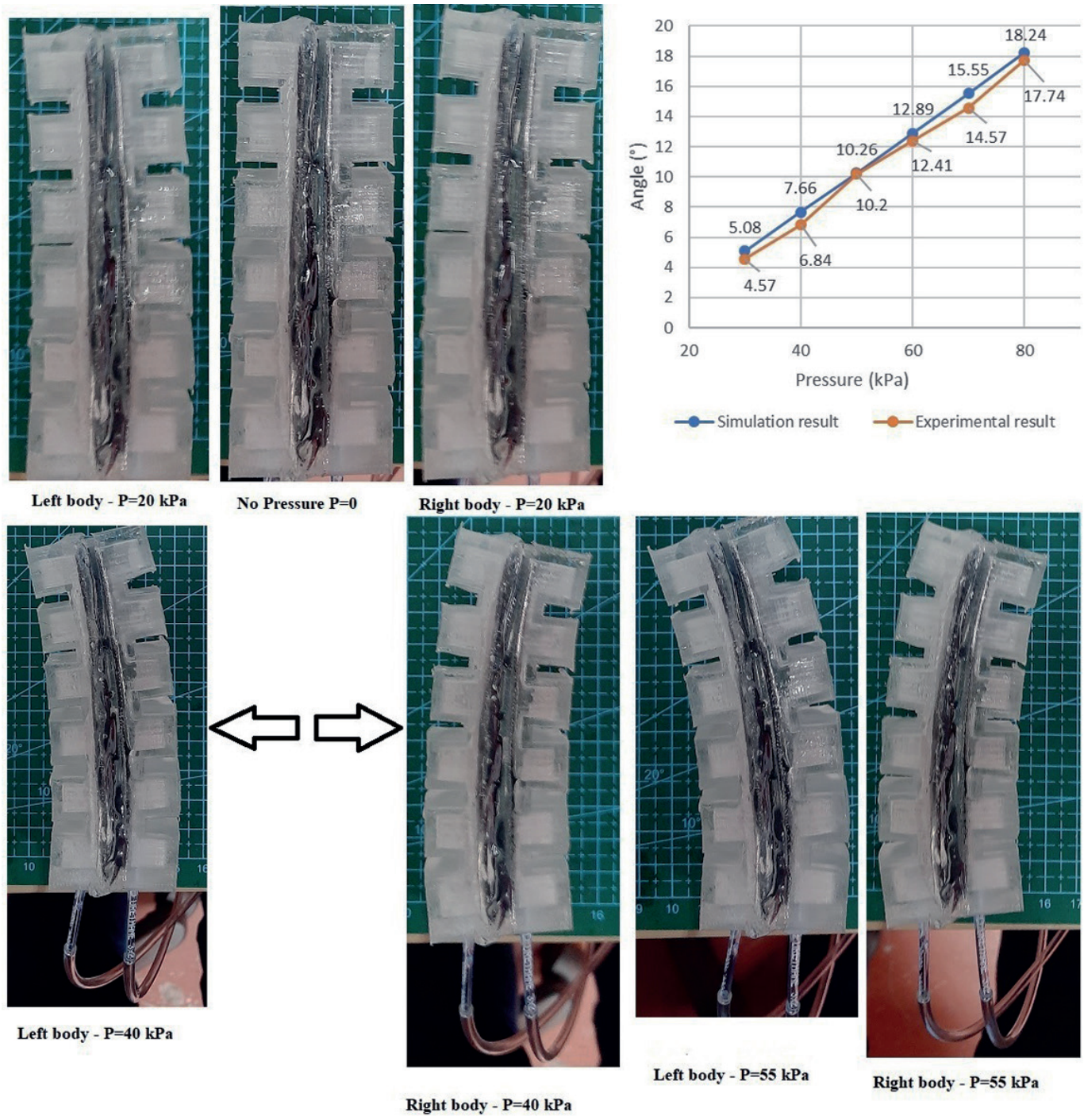

Fig. 8b. Testing of body actuator at different pressures

3. Results and discussion

The results from the parametric study, MATLAB simulation and experimental results are presented in this section. Figure 9 shows the bending angle measured from simulation and experiments.

An acceptable difference is noticed between simulation and experimental results. Numerically, the mean difference in the bending angle for 20 to 90 kPa of air input into the limb actuator is 0.89°. The numerical difference in the bending angle measured from the body actuator is 0.478°. Figure 10 shows the motion of the salamander robot.

The salamander robot is able to successfully walk on ground with the velocity of 0.06774 m/s. In Faudzi *et al.* [13], McKibben muscles were used for the design of the salamander robot and it was able to walk at the velocity of 0.056 m/s on a flat

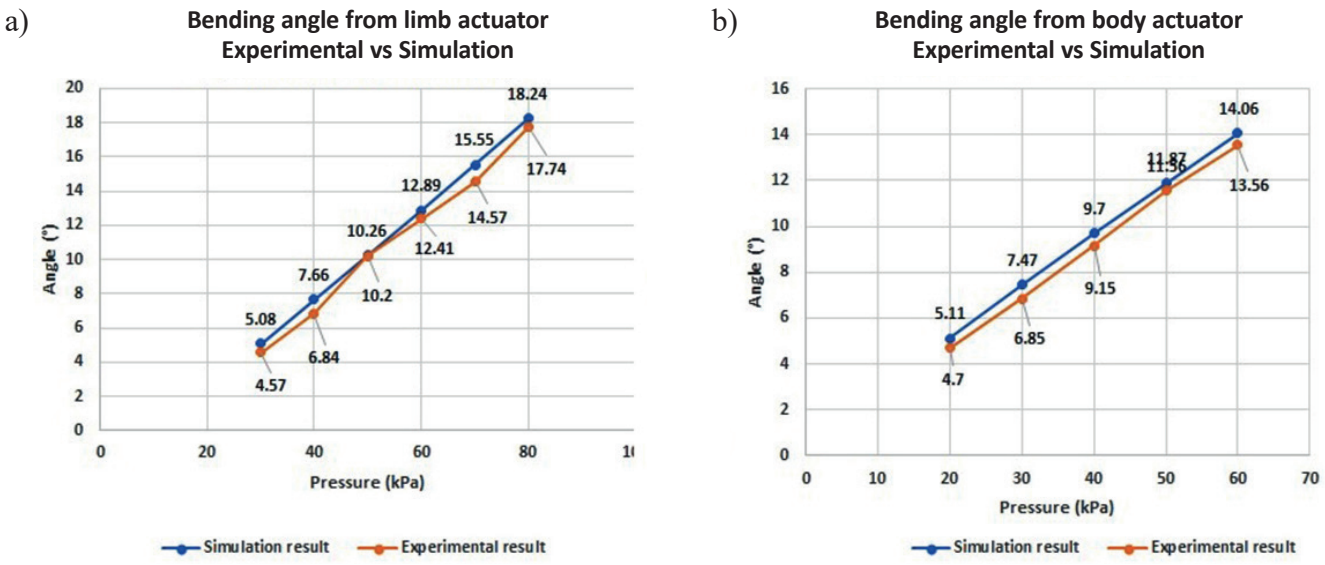

Fig. 9. Bending angle (a) measured from limb soft actuator and (b) measured from body soft actuator

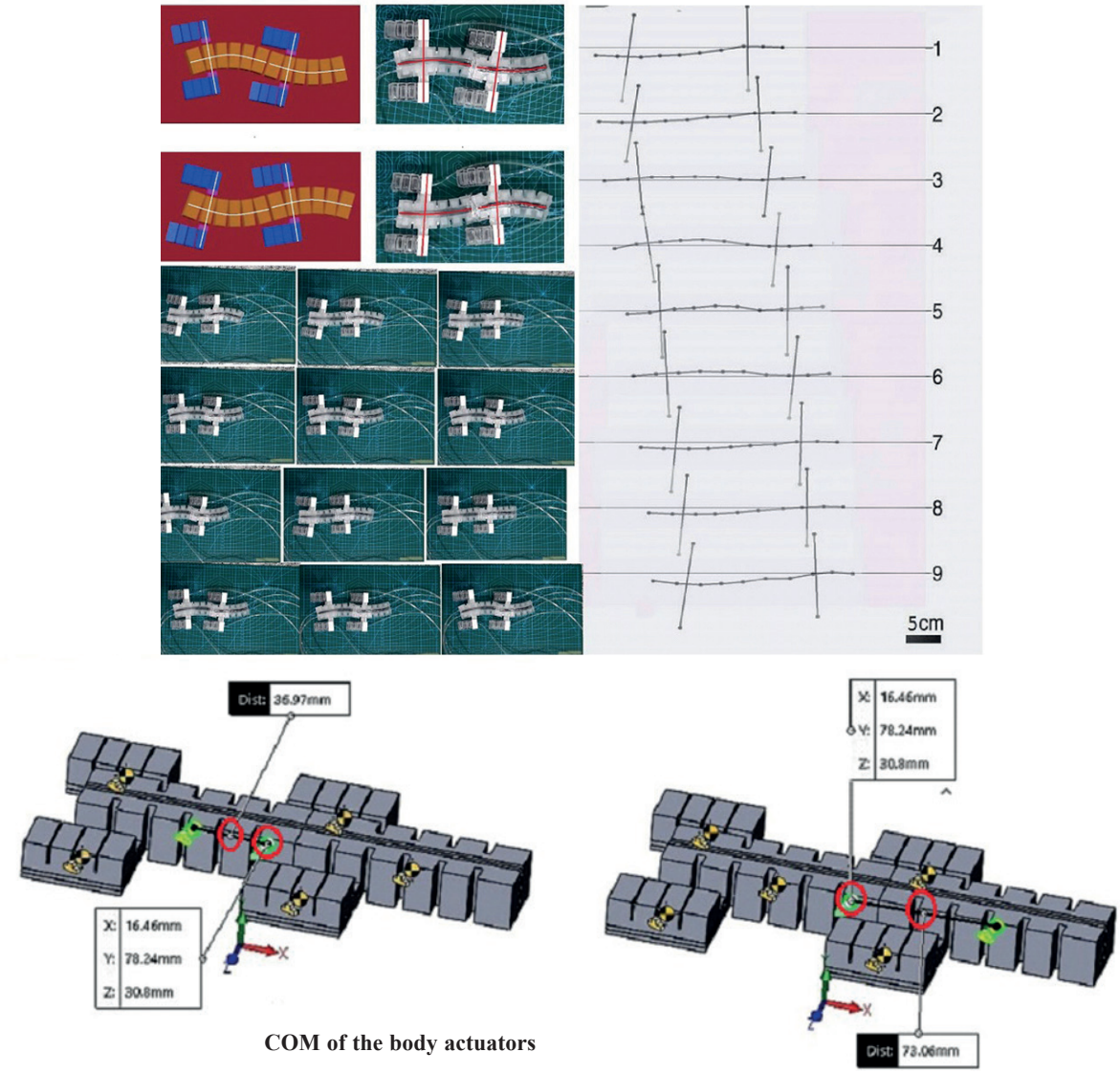

Fig. 10. Motion of the salamander robot (see also the video of the robot attached)

plane and on one inclined by 10°. The velocity of the current robot is faster than that of Faudzi *et al.* [13]. The velocity of the current robot moving in simulated physics is 0.07045 m/s at 10 seconds. The difference between the experimental results and simulation is 3.85%. Though the error is within the limit, the gait must be improved by having a more accurate bending angle, such as is seen in the simulation. The fabricated robot tends to bend slightly towards the right while it is very straight in numerical simulation. In the MATLAB simulation, the body and limb were attached by means of a solid joint (pink color block in Fig. 6). When the body of the salamander bent, the limb also bent to a certain angle with the help of the solid joint and hence formed a straight line perpendicular to its body. But, in the current robot prototype, the joint was done with Silicone KE-1603, which is the same material as the one used for fabricating the soft actuator. It does not seem to be a completely solid joint and it tends to bend along the body. It could be the reason for the error in the bending angle and gait. The issue observed would be corrected in the next version of our prototype, which aims to design the salamander robot for walking and swi mming. The center of mass (COM) of the body actuators is located at the distance of 36.97 mm and 73.06 mm from ($x = 16.46$ mm, $y = 78.24$ mm, $z = 30.8$ mm), respectively.

4. Conclusions

Mimicking of the movement of the salamander was attempted with PneuNet soft actuators. The design of the salamander robot was carried out through a parametric study followed by MATLAB numerical simulation. The best parameters to design both limb and body actuators were selected from the model which produced the highest bending angle. The height of chambers and wall thickness for both limb and body actuators were 15 mm and 2.5 mm, respectively. The number of chambers were 4 for the limb actuator and 6 for the body actuator. The distance between the chamber was 1 for the limb actuator and 4 for the body actuator. The final model of the salamander robot was done with these parameters and the numerical simulation was conducted using Simscape Multibody in the Simulink tool. The fastest walking gait was produced by 1Hz frequency for the limb and body, 0.3 second signal delay for the limb actuator and negative π phase difference for every contralateral side of the limb. The prototype of the salamander robot was developed using the Shin-Etsu KE-1603 material. Rigorous tests on the motion of the robot were conducted with a sine-based controller. The developed salamander robot was able to move following an almost identical pattern to that from the simulation with 0.0677 m/s. The error in velocity between actual and numerical simulation is 3.85%, which we shall aim to correct in our next version of the salamander robot.

Funding: This work is supported by the Fundamental Research Grant Scheme (FRGS) with project code FRGS/1/2019/TK04/UCSI/02/1 awarded by the Ministry of Higher Education, Malaysia, and Universiti Teknologi Malaysia Research University Grant, Project No. Q.J13 0000.2409.08G31.

Conflict of interest: The authors do not have any conflict of interest.

References

[1] A.J. Ijspeert, "Central pattern generators for locomotion control in animals and robots: A review", *Neural Netw.* 21, 642–653 (2008).

[2] K. Karakasiliotis, N. Schilling, J.C. Auke, and J. Ijspeert, "Where are we in understanding salamander locomotion : biological and robotic perspectives on kinematics", *Biol. Cybern.* 107, 529–544 (2012).

[3] J. Cabelguen, C. Bourcier-Lucas, and R. Dubuc, "Bimodal Locomotion Elicited by Electrical Stimulation of the Midbrain in the Salamander Notophthalmus viridescens", *J. Neurosci.* 23(6), 2434–2439 (2003).

[4] J.L. Edwards, "The Evolution of Terrestrial Locomotion", in *Major Patterns in Vertebrate Evolution*, pp. 1961–1962, Edition. no 1955, Plenum Press, New York, 1977.

[5] A. Ross, "Hindlimb Kinematics During Terrestrial Locomotion in a Salamander (Dicamptodon Tenebrosus)", *J. Exp. Biol.* 193(1), 255–83 (1994).

[6] A.J. Ijspeert, G.A. Ascoli, and D.N. Kennedy, "Simulation and Robotics Studies of Salamander Locomotion", *Neuroinformatics* 3, 171–195 (2005).

[7] K. Karakasiliotis and A.J. Ijspeert, "Analysis of the terrestrial locomotion of a salamander robot", in *The 2009 IEEE/RSJ International Conference on Intelligent Robots and Systems*, 2009, pp. 5015–5020.

[8] A.J. Ijspeert, A. Crespi, D. Ryczko, and J. Cabelguen, "From Swi mming to Walking with a Spinal Cord Model", *Science* 315, 1416–1421 (2007).

[9] A. Bicanski *et al.*, "Decoding the mechanisms of gait generation in salamanders by combining neurobiology, modeling and robotics", *Biol. Cybern.* 107, 545–564 (2013).

[10] Q. Liu, H. Yang, J. Zhang, and J. Wang, "A new model of the spinal locomotor networks of a salamander and its properties", *Biol. Cybern.* 112(4), 369–385 (2018).

[11] Q. Liu, Y. Zhang, J. Wang, H. Yang, and L. Hong, "Modeling of the neural mechanism underlying the terrestrial turning of the salamander", *Biol. Cybern.* 114, 317–336 (2020).

[12] C. Zhou, M. Tan, N. Gu, Z. Cao, S. Wang, and L. Wang, "The Design and Implementation of a Biomimetic Robot Fish", *Int. J. Adv. Robot. Syst.* 5(2), 185–192 (2008).

[13] A.A.M. Faudzi, M.R.M. Razif, G. Endo, H. Nabae, and K. Suzumori, "Soft-Amphibious Robot using Thin and Soft McKibben Actuator", in *2017 IEEE International Conference on Advanced Intelligent Mechatronics (AIM)*, 2017, pp. 981–986.

[14] N. Ili, M.R. Muhammad Razif, A.M. Faudzi, E. Natarajan, K. Iwata, and K. Suzumori, "3-D finite-element analysis of fiber-reinforced soft bending actuator for finger flexion", *2013 IEEE/ASME Int. Conf. Adv. Intell. Mechatronics Mechatronics Hum. Wellbeing, AIM 2013*, 2013, pp. 128–133.

[15] M.R.M. Razif, A.A.M. Faudzi, M. Bavandi, N.A.M. Nordin, E. Natarajan, and O. Yaakob, "Two chambers soft actuator realizing robotic gymnotiform swi mmers fin", *2014 IEEE Int. Conf. Robot. Biomimetics, IEEE ROBIO 2014*, 2014, pp. 15–20.

[16] N. Elango and A.A.M. Faudzi, "A review article: investigations on soft materials for soft robot manipulations", *Int. J. Adv. Manuf. Technol.* 80, 1027–1037 (2015).

[17] Y. Nishioka, M. Uesu, H. Tsuboi, S. Kawamura, T. Yasuda, and M. Yamano, "Development of a pneumatic soft actuator with pleated inflatable structures", *Adv. Robot.* 31(14), 753–762 (2017).

[18] Z. Wang, P. Polygerinos, J.T.B. Overvelde, K.C. Galloway, K. Bertoldi, and C.J. Walsh, "Interaction Forces of Soft Fiber Reinforced Bending Actuators", *IEEE/ASME Trans. Mechatron.* 22(2), 717–727 (2017).

[19] A. Ning, M. Li, and J. Zhou, "Modeling and understanding locomotion of pneumatic soft robots", *Soft Mater.* 16(3), 151–159 (2018).

[20] W. Hu, W. Li, and G. Alici, "3D Printed Helical Soft Pneumatic Actuators", in *2018 IEEE/ASME International Conference on Advanced Intelligent Mechatronics (AIM)* 2018, pp. 950–955.

[21] S. Furukawa, S. Wakimoto, T. Kanda, and H. Hagihara, "A Soft Master-Slave Robot Mimicking Octopus Arm Structure Using Thin Artificial Muscles and Wire Encoders", *Actuators* 8(40), 1–13 (2019).

[22] V. Cacucciolo, J. Shintake, Y. Kuwajima, S. Maeda, D. Floreano, and H. Shea, "Stretchable pumps for soft machines", *Nature* 572, 516–519 (2019).

[23] M.A. Robertson, O.C. Kara, and J. Paik, "Soft pneumatic actuator-driven origami-inspired modular robotic 'pneumagami'", *Int. J. Robot. Res.* 40(1), 72–85 (2020).

[24] E. Natarajan, "Evaluation of a Suitable Material for Soft Actuator Through Experiments and FE Simulations", *Int. J. Manuf. Mater. Mech. Eng.* 10(2), 64–76 (2020).

[25] B. Mosadegh, P. Polygerinos, Ch. Keplinger, S. Wennstedt, R.F. Shepherd, U. Gupta, J. Shim, K. Bertoldi, C.J. Walsh, and G.M. Whitesides, "Pneumatic Networks for Soft Robotics that Actuate Rapidly", *Adv. Funct. Mater.* 2014(24), 2163–2170 (2014).

[26] T. Wang, L. Ge, and G. Gu, "Progra mmable design of soft pneu-net actuators with oblique chambers can generate coupled bending and twisting motions", *Sens. Actuator A-Phys.* 217, 131–138 (2018).

[27] P. Boyraz, G. Runge, and A. Raatz, "An Overview of Novel Actuators for Soft Robotics", *Actuators* 7(48), 1–21 (2018).

[28] M. Manns, J. Morales, and P. Frohn, "Additive manufacturing of silicon based PneuNets as soft robotic actuators", *Procedia CIRP* 72, 328–333 (2018).

[29] Y. Sun, Q. Zhang, X. Chen and H. Chen, "An Optimum Design Method of Pneu-Net Actuators for Trajectory Matching Utilizing a Bending Model and GA", *Math. Probl. Eng.* 2019, 6721897 (2019), doi: 10.1155/2019/6721897.

[30] T. Zielinska, "Autonomous walking machines–discussion of the prototyping problems", *Bull. Pol. Acad. Sci. Tech. Sci.* 58(3), 443–451 (2010), doi: 10.2478/v10175-010-0042-2.